Hydrodynamic interaction effects in the rheological properties of Hookean dumbbells in steady shear flow: a Brownian dynamics simulation study

F. G. Díaz and J. García de la Torre*
Department of Chemical Physics, Faculty of Science, Chemistry and Mathematics, Universidad de Murcia, 30001 Murcia, Spain

and J. J. Freire
Department of Chemical Physics, Faculty of Chemistry, Universidad Complutense, 28040 Madrid, Spain
(Received 27 May 1988; accepted 27 June 1988)

In this paper we present a Brownian dynamics simulation study where we employ the algorithm of Ermak and McCammon including solvent flow in the calculation of the rheological properties of Hookean dumbbells in steady shear flow. We have also included the possibility of the excluded volume and we have studied several possibilities with and without hydrodynamic interactions (HI). When hydrodynamic interaction is rigorously treated, the intrinsic viscosity is found to increase. If the Rotne–Prager–Yamakawa HI tensor is used instead of the Oseen tensor, the changes in the material functions are quite small. On the other hand, excluded-volume interactions produce, as expected, an increase in the viscosity. This is so both with and without HI. Our results are compared with those of other works in which the HI tensor is pre-averaged or consistently averaged.

(Keywords: interaction effects; rheology; shear flow; Brownian dynamics)

INTRODUCTION

In the theoretical description of rheological properties of polymer solutions there is a complex interplay between chain statistics, solution flow and hydrodynamic interactions (HI). It can be learned from standard monographs[1,2] that HI effects have been traditionally neglected or treated in approximate ways such as by pre-averaging procedures. Recently, the increasing availability of computing power has stimulated the development of simulation procedures for polymer dynamics, which are either of the Monte Carlo[3,4] or the Brownian dynamics (BD)[5,6] type. While Monte Carlo techniques are appropriate for translational diffusion and even the zero-shear intrinsic viscosity, BD simulation seems the proper choice for rheological properties. Indeed, BD has already been applied to study the non-equilibrium statistics of model chains in shear flows[7–11], although neglecting HI effects.

On the other hand, there have been recent attempts to improve the approximate inclusion of HI (via averaging) in the description of shear behaviour. Thus, Öttinger[12–14] has included consistently averaged HI at the Oseen level[2] in the dynamics of the simplest model, the Rouse or Hookean dumbbell[15,16], and López de Haro and Rubi[17] have gone beyond the Oseen level to consider the influence of finite bead size[18–21]. A direct, numerical solution of the diffusion equation for dumbbells, with non-pre-averaged Oseen HI, has been presented by Fan[22]. Analytical results with HI are available only for zero shear rate[23,24].

In this Paper we employ the Brownian dynamics simulation algorithm of Ermak and McCammon[5,25–27], including solvent flow[28], in the calculation of the material functions of Hookean dumbbells in steady shear flow. We consider several possibilities regarding HI, and the results are compared with those from the analytical and numerical studies mentioned above.

METHODS

Our polymer model is the simple Hookean dumbbell, which has two spherical beads with radius σ and friction coefficient $\zeta = 6\pi\eta_0\sigma$, where η_0 is the viscosity of the solvent. We consider identical beads for simplicity, although there is no restriction in this regard. The beads are joined by an elastic connector to which a force

$$\boldsymbol{F} = H\boldsymbol{R} \tag{1}$$

is associated, where $\boldsymbol{R}$ is the vector joining the centres of the beads and H is the spring constant. If $\boldsymbol{r}_1$ and $\boldsymbol{r}_2$ are the position vectors of the beads, we have $\boldsymbol{R} = \boldsymbol{r}_2 - \boldsymbol{r}_1$. In the absence of flow, the equilibrium mean squared distance between beads is

$$\langle R^2 \rangle_0 \equiv b^2 = 3k_B T/H \tag{2}$$

* To whom correspondence should be addressed

0032-3861/89/020259-06$03.00

where k_BT is the Boltzmann factor. A characteristic time is usually defined as

$$\lambda_H = \zeta/4H = \pi\eta_0\sigma b^2/2k_BT \quad (3)$$

The motion of the polymer model is governed by the stochastic differential equation of Langevin. The reader is referred to reference 29 for useful general information on this type of equation. Although sophisticated algorithms for stochastic differential equations are available, we have chosen for this work the simple algorithm proposed by Ermak and McCammon[5,26,27]. In this procedure, which has a fixed time step Δt, the equation of motion is

$$\boldsymbol{r}_i = \boldsymbol{r}_i^o + \frac{\Delta t}{k_BT}\sum_j \boldsymbol{D}_{ij}^o \cdot \boldsymbol{F}_j^o + \Delta t \sum_j \left(\frac{\partial \boldsymbol{D}_{ij}}{\partial \boldsymbol{r}_j}\right)^o + \Delta t \boldsymbol{v}(\boldsymbol{r}_i^o) + \rho_i^o(\Delta t) \qquad i,j = 1,2 \quad (4)$$

The superscript o in $\boldsymbol{r}_i^o$ and elsewhere refers to the instant at which the time step begins. $\boldsymbol{D}^o_{ij}$ is the ij block of the diffusion tensor, and $\boldsymbol{F}_1^o = -\boldsymbol{F}_2^o = H(\boldsymbol{r}_2^o - \boldsymbol{r}_1^o).\boldsymbol{v}(\boldsymbol{r}_i^o)$ is the velocity of the solvent at the centre of the bead. For steady shear flow, $v_x = y_i^o\dot{\gamma}$, $v_y = v_z = 0$, where $\dot{\gamma}$ is the shear rate. ρ_i is a Gaussian random vector with zero mean and a variance–covariance matrix given by

$$\langle \rho_i^o(\Delta t)\rho_j^o(\Delta t)\rangle = 2\Delta t \boldsymbol{D}_{ij}^o \quad (5)$$

If HI is neglected, one has

$$\boldsymbol{D}_{ii}^o = (k_BT/\zeta)\boldsymbol{I} \quad (6)$$

and $\boldsymbol{D}_{ij}^o = \boldsymbol{O}$ for $i \neq j$. The gradient term is also zero and equation (4) reduces to

$$\boldsymbol{r}_i = \boldsymbol{r}_i^o + (\Delta t/\zeta)\boldsymbol{F}_i^o + \rho_i^o(\Delta t) \quad (7)$$

which is the algorithm used by Dotson and co-workers[8,9,11].

At the next level, HI can be described by the Oseen tensor. Then $\boldsymbol{D}_{ii}$ is given by equation (6) and for $i \neq j$ we have

$$\boldsymbol{D}_{ij} = (k_BT/8\pi\eta_0 R)(\boldsymbol{I} + \boldsymbol{RR}/R^2) \quad (8a)$$

or

$$\boldsymbol{D}_{ij} = h^*(\pi/3)^{1/2}(3k_BT/4\zeta)(b/R)(\boldsymbol{I} + \boldsymbol{RR}/R^2) \quad (8b)$$

where

$$h^* = (3/\pi)^{1/2}\zeta/6\pi\eta_0 b \quad (9)$$

is the usual HI parameter with values $0 \leqslant h^* \lesssim 0.3$, with $h^* = 0$ when HI is neglected. If the beads are Stokes spheres, as it is assumed throughout this Paper, then $h^* = (3/\pi)^{1/2}\sigma/b$. Finally, we note that $\partial \boldsymbol{D}_{ij}/\partial \boldsymbol{r}_j$ is also zero for Oseen tensors. It is well known that the Oseen tensor is not positive definite at small distances $R < 2\sigma$. In that case the gradient is given by equation (7) in Reference 27.

At the following level, the influence of the finite size of beads in the HI is accounted for by means of Rotne–Prager–Yamakawa[18,19] tensors. $\boldsymbol{D}_{ii}$ is again given by equation (6) and, for non-overlapping beads ($R \geqslant 2\sigma$), we have

$$\boldsymbol{D}_{ij} = h^*(\pi/3)^{1/2}(3k_BT/4\zeta)(b/R) \times [\boldsymbol{I} + \boldsymbol{RR}/R^2 + (2\sigma^2/3R^2)(\boldsymbol{I} - 3\boldsymbol{RR}/R^2)] \quad (10)$$

with zero gradient. If the beads are allowed to overlap ($R < 2\sigma$), the Rotne–Prager tensor[19] is

$$\boldsymbol{D}_{ij} = (k_BT/\zeta)[(1 - 9R/32\sigma)\boldsymbol{I} + (3/32\sigma)\boldsymbol{RR}/R^2)] \quad (11)$$

Although no restriction has to be placed in principle on the interbead distance R, one may wish to evaluate excluded volume effects by forbidding conformations with overlapping beads. To do so, if the values of $\boldsymbol{r}_1$ and $\boldsymbol{r}_2$ after a time step (equation (7)) are such that $R < 2\sigma$, with an overlap $e = 2\sigma - R$, additional displacements $-(e/R)\boldsymbol{R}$ and $(e/R)\boldsymbol{R}$ are added to $\boldsymbol{r}_1$ and $\boldsymbol{r}_2$, respectively. These displacements do not move the centre of the dumbbell and do not change its orientation, and are the same as those produced by a hypothetical hard-spheres collision during the step.

In the simulation work it is useful to work with dimensionless quantities. The following normalization factors are used: length, b; translational friction, $\zeta \equiv 6\pi\eta_0\sigma$; energy, k_BT; translational diffusion $k_BT/6\pi\eta_0\sigma$; time, $6\pi\eta_0\sigma b^2/k_BT$; and shear rate, $k_BT/6\pi\eta_0\sigma b^2$. In this way we have (numerically) $b = 1$, $k_BT = 1$, $\zeta = 1$, $H = 3$, $\lambda_H = 1/12$, $\sigma = 1.023h^*$. The time step must be small enough so that the force and the diffusion tensor do not change appreciably during the step. This is the practical condition of validity of equation (4). However, it should also be as large as possible so that for a given number of steps the trajectory is long enough. We have found empirically that $\Delta t = 0.01$ in the above units is a convenient choice. Typically, the simulated trajectories were composed of 5×10^5 steps, divided into 25 sub-trajectories of 2×10^4 steps. The averages of properties were computed for each subtrajectory, and from them we evaluated the trajectory averages and their statistical uncertainties.

The primary rheological property is the stress tensor, given by the Kramers expression[1]

$$\tau = -\eta_0\dot{\gamma} - n\langle \boldsymbol{RF}\rangle + nk_BT\boldsymbol{I} \quad (12)$$

For simple shear flows, all the components of the $\dot{\gamma}$ tensor are zero except $\dot{\gamma}_{xy} = \dot{\gamma}_{yx} \equiv \dot{\gamma}$. n is the number density of polymer molecules, $\boldsymbol{I}$ the unit tensor and $\langle \ldots \rangle$ denotes an ensemble average that in the simulation work is identified with the trajectory average. From the stress tensor we obtain the material functions, namely the viscosity

$$\eta \equiv -\tau_{xy}/\dot{\gamma} = \eta_0 + n\langle R_xF_y\rangle/\dot{\gamma} \quad (13)$$

and the first and second normal stress coefficients,

$$\Psi_1 = n[\langle R_xF_x\rangle - \langle R_yF_y\rangle]/\dot{\gamma}^2 \quad (14)$$

$$\Psi_2 = n[\langle R_yF_y\rangle - \langle R_zF_z\rangle]/\dot{\gamma}^2 \quad (15)$$

Equations (13)–(15) follow directly from equation (12) and the definition of the material functions. For the Hookean dumbbell considered in this work one makes the additional simplification of substituting $\langle \boldsymbol{RF}\rangle = H\langle \boldsymbol{RR}\rangle$. Thus, all the material functions can be extracted from the tensor $\langle \boldsymbol{RR}\rangle$, whose trace is the mean squared end-to-end distance, $\langle R^2\rangle = \mathrm{tr}\langle \boldsymbol{RR}\rangle$.

RESULTS AND DISCUSSION

Figure 1 displays the BD simulation results obtained for $\langle R^2\rangle$ as a function of reduced shear rate. If HI is

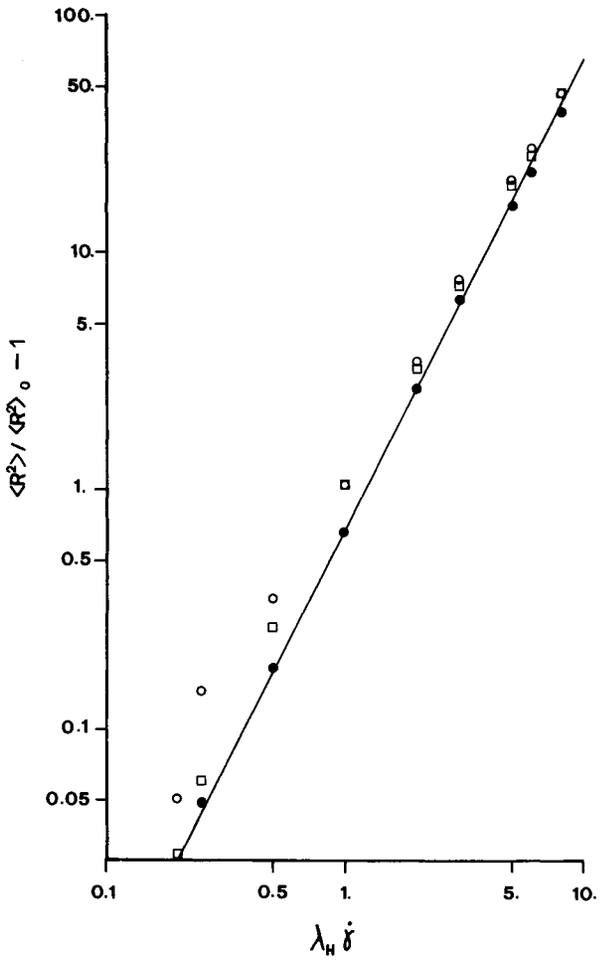

Figure 1 Relative increase of end-to-end distance *versus* reduced shear rate $\lambda_H\dot{\gamma}$. ——, Prediction of equation (16b). BD results are: ●, without HI; ○, with Oseen HI; □, with Rotne–Prager–Yamakawa HI. The HI parameter is $h^*=0.25$

neglected, $\langle R^2\rangle$ can be predicted analytically by means of the equation of Bird *et al.*[7] for a Rouse chain with N beads particularized for $N=2$:

$$\langle R^2\rangle/\langle R^2\rangle_0 = 1+(1/45)N(N+1)(N^2+1)\lambda_H^2\dot{\gamma}^2 \quad (16a)$$

$$= 1+(2/3)\lambda_H^2\dot{\gamma}^2 \qquad (N=2) \qquad (16b)$$

where $\langle R^2\rangle_0$ is the zero-shear-rate value. As shown in *Figure 1* our BD results without HI, which are equivalent to those of Dotson[8], are in perfect agreement with equation (16b).

The effect of HI is more clearly shown in *Figure 2*, where the ratio of $\langle R^2\rangle$ values with and without HI is presented as a function of shear rate. In general, HI produces an expansion of the dumbbell in the whole range of shear rate. The trend of this effect is early reasoned. At very low shear rate $\langle R^2\rangle_{HI}$ and $\langle R^2\rangle_{no\ HI}$ are both very close to $\langle R^2\rangle_0$ and their ratio is close to one. On the other hand, at very high shear rate the two beads are well separated and the HI effect will be very weak, so that $\langle R^2\rangle_{HI} \approx \langle R^2\rangle_{no\ HI}$, with a ratio approaching unity again. Thus, one expects a maximum that, as shown in *Figure 2*, takes place at $\lambda_H\dot{\gamma}\approx 1$ with $\langle R^2\rangle_{HI}/\langle R^2\rangle_{no\ HI}\approx 1.25$. At low shear rate, the increase in $\langle R^2\rangle$ is more pronounced for the Oseen tensor. At higher rates the results for both tensors coincide within the statistical uncertainty of the simulation.

The intrinsic viscosity results are presented in *Figure 3*, where we have actually plotted the ratio

$$[\eta]^* = (\eta-\eta_0)/nk_BT\lambda_H \qquad (17)$$

so that if HI is neglected $[\eta]^*=1$ independently of shear rates. We see in *Figure 3* that our BD simulation results without HI follow this theoretical prediction well, within statistical error, except for a small, apparently systematic deviation that appears at very low shear rate. We note how the simulation error increases with decreasing shear rate. This is so because $\langle R_xF_y\rangle$ goes to zero proportionally to $\dot{\gamma}$.

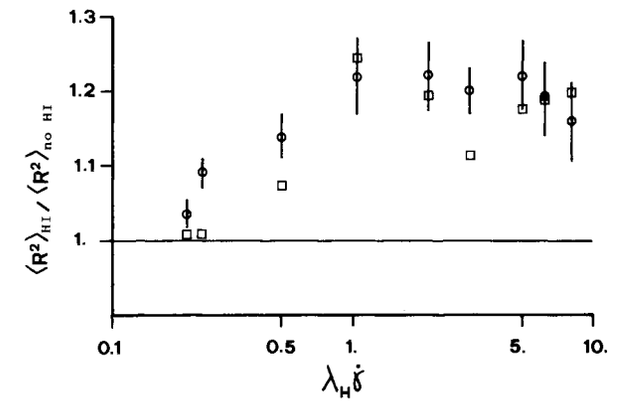

Figure 2 Ratio of $\langle R^2\rangle_{HI}$ (with HI) to $\langle R^2\rangle_{no\ HI}$ (without HI) *versus* $\lambda_H\dot{\gamma}$. ○, Oseen HI; □, Rotne–Prager–Yamakawa HI ($h^*=0.25$). The error bars are for the Oseen HI results. The errors of the other set of results are similar

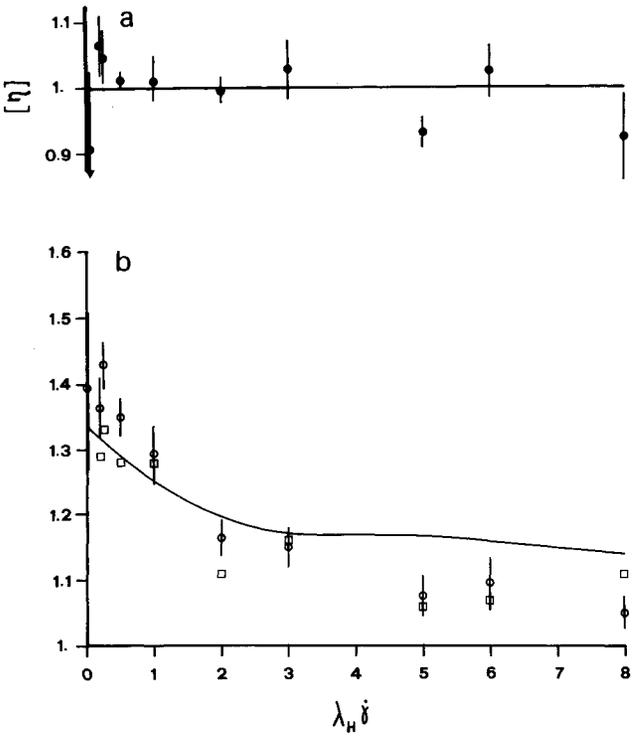

Figure 3 Intrinsic viscosity $[\eta]$, normalized to the value without hydrodynamic interaction, *versus* shear rate. (a) Simulation results without HI. (b) BD results with (○) Oseen and (□) Rotne–Prager–Yamakawa tensors. ——, Numerical solution of the diffusion equation obtained by Fan[22]

The BD results with HI are also displayed in *Figure 3*, along with those from the numerical solution of the diffusion equation with the Oseen tensor obtained by Fan[22]. Taking the latter as reference, our BD results with Oseen interaction are found to be in semi-quantitative agreement. At low $\dot{\gamma}$, the BD simulation seems to overestimate $[\eta]$ by about 5% (as happened for the no-HI case), and for high $\dot{\gamma}$ the simulation results are about 10% below those of Fan[22]. The discrepancies between our BD results and the numerical results of Fan are of the same order as those found for BD values of translational diffusion coefficients and rotational relaxation times of rigid dumbbells and trimers[27]. The $\dot{\gamma}=0$ value given by Fan coincides with the analytical result of Pyun[23], $[\eta]^*=(1-0.990h^*)^{-1}$, with $[\eta]^*=1.33$ for $h^*=0.25$. Although it would be desirable to run BD simulations with smaller Δt and longer trajectories, our results, at least, demonstrate the validity of the BD simulation technique for evaluating material functions and predicting semi-quantitatively their shear-rate dependence.

Results for the first normal coefficient, normalized to the value with no HI, as before,

$$\Psi_1^*=\Psi_1/2nk_BT\lambda_H^2 \tag{18}$$

are plotted in *Figure 4*. The trend of the results is very similar to that of the intrinsic viscosity. We also obtained results for the second normal coefficient. Owing to the statistical error of the simulation, we could not detect a systematic departure from the no HI result, $\Psi_2=0$.

The moderate time step used in the simulation could cause some error in the resulting values of the material functions. With $\Delta t=0.01$, one would estimate an error of some 3% for Ψ_1[30]. This situation could be more noticeable at high shear rates. For instance, for $\lambda_H\dot{\gamma}=5$, with $\lambda_H=1/12$ (in reduced units), the relevant time scale is $\lambda^{-1}=0.017$, and our time step is not much smaller than this. The errors caused by our simple, fixed-step method are difficult to estimate. We recall, however, that the results without HI agree within simulation error with the theoretical prediction or expected behaviour (*Figures 3–5*). Since the problem is independent of HI, we think that our results are, in general, valid for the discussion that follows.

To ascertain the influence of the excluded volume (EV) effect, simulations with hard spheres and without HI were carried out as described above. The results are presented in *Figure 5*. It is clear that the hard-spheres restriction produces an increase of the material functions at low or moderate shear rate (up to about 10% in $[\eta]$ and 20% in Ψ_1), and is negligible at higher rates.

We recall the well known result[1] that when hydrodynamic interactions are described by the pre-averaged Oseen tensor, $\boldsymbol{D}_{ij}=(k_BT/6\pi\eta_0R)\boldsymbol{I}$, the material functions turn out to be shear rate independent, given by $[\eta]^*=(1-2^{\frac{1}{2}}h^*)^{-1}$, $\Psi_1^*=(1-2^{\frac{1}{2}}h^*)^{-2}$ and $\Psi_2^*=0$.

Figure 6 summarizes the results for the shear rate dependence of the intrinsic viscosity obtained in various treatments. Lines a and f correspond to the results without HI and with pre-averaged HI, respectively, in the absence of EV. Curve b represents the trend followed by the no HI results with excluded volume that were displayed in *Figure 5*. The results of Fan[22], with Oseen

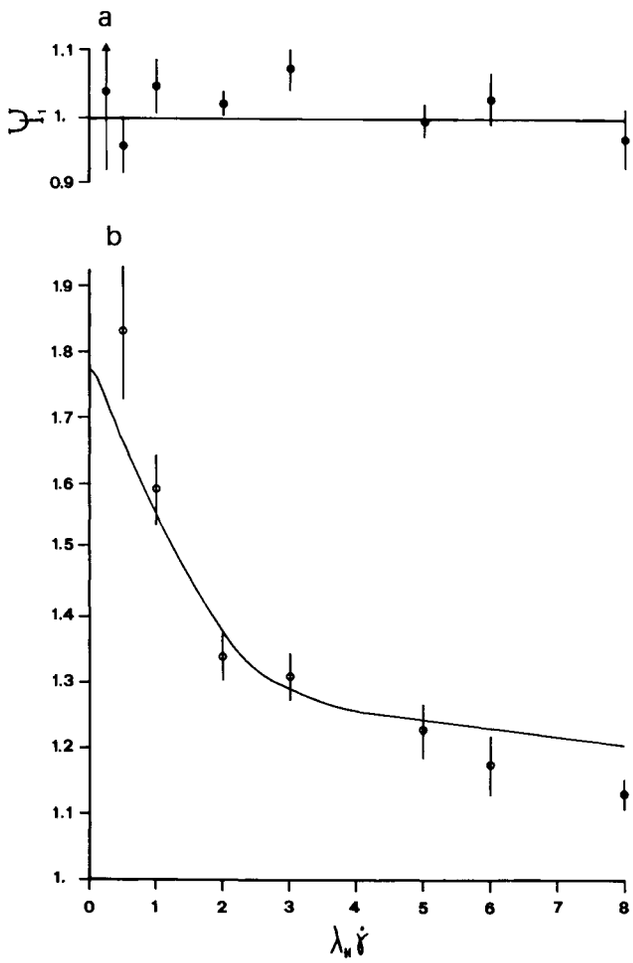

Figure 4 As for *Figure 3* for the first normal stress coefficient, Ψ_1^*

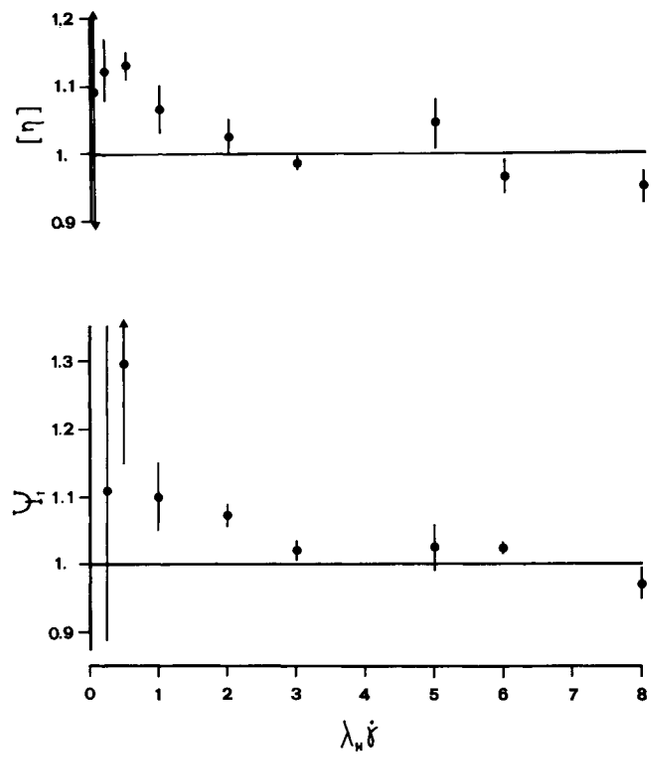

Figure 5 Simulation results for $[\eta]$ and Ψ_1 versus $\lambda_H\dot{\gamma}$ for dumbbells with hard, non-overlapping spheres ($R>2\sigma$) and without HI

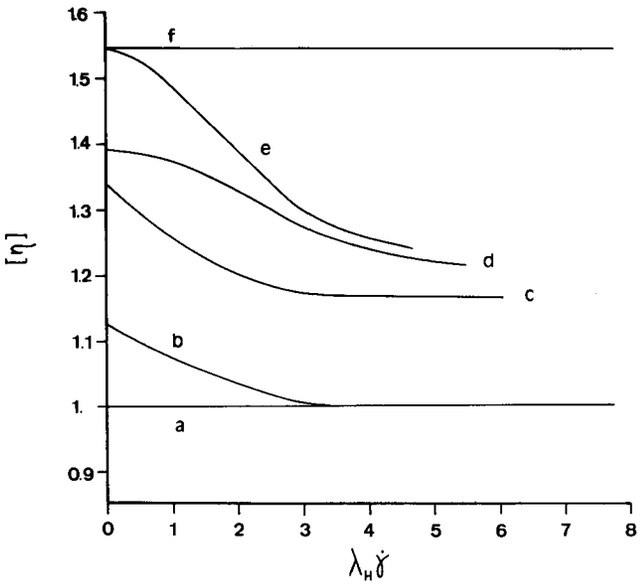

Figure 6 Variation of viscosity with shear rate for dumbbells with $h^* = 0.25$, according to various treatments. a, No HI, no EV; b, no HI, EV (this work); c, OS (RPY), no EV (Reference 22, this work); d, CA, RPY, EV[17]; e, CA, OS, no EV[12]; f, PA, OS, no EV. Codes: no HI, without hydrodynamic interaction; OS, Oseen interaction; RPY, Rotne–Prager–Yamakawa interaction; PA, pre-averaging; CA, consistent averaging; EV, excluded volume

interaction, are given by curve c, which also represents our BD simulation results with the Oseen and the modified (Rotne–Prager–Yamakawa) tensors. Curves d and e are those obtained with the consistent averaging procedure; e is for Oseen interaction without EV[12] and d is for the modified tensor and EV[17].

From the works of Pyun and Fixman[23,24] on the zero shear rate viscosity and Fan[22] on the shear rate dependence, we know that hydrodynamic interaction at its lowest (Oseen) level causes an increase in $[\eta]$ over the no HI value and a non-Newtonian, shear rate dependent behaviour. This situation is illustrated by comparing curves a and c in *Figure 6*. Our simulation results indicate that the improvement in HI introduced by the Rotne–Prager–Yamakawa tensor has quite a small influence. It seems, therefore, that the Oseen description is acceptable.

In their consistent average treatment, López de Haro and Rubí[17] included a hard-sphere, excluded-volume effect as a natural complement to the consideration of finite bead size by means of the modified interaction tensor. It is not clear to what extent the EV refinement can be relevant in a very idealized polymer model such as the Hookean dumbbell. Overlooking this point, we see that the bare EV effect (in the absence of HI) produces, as shown by curves a and b in *Figure 6*, the onset of non-Newtonian behaviour and an increase in $[\eta]$. The latter fact was expected, since the most immediate consequence of EV is an increase in the particle's dimension, and this should cause an increase in $[\eta]$ at low shear rate. For high shear rate, the dumbbell is much more elongated, the distance R is, on the average, much greater than the size 2σ and the EV effect is negligible.

To check the influence of EV in the presence of HI, we carried out a few simulations with the Oseen tensor and hard-spheres interaction. The results (not shown in *Figure 3*) are slightly (roughly 10%) higher than those with Oseen tensor and without EV at low shear rates, while at higher shear rates the results with and without EV effect coincide within statistical error. Thus the influence of EV displayed in *Figures 5* and *6* does not depend on the inclusion of HI.

It is also well known that pre-averaging of the hydrodynamic interaction gives a value for $[\eta]$ which is too high and shear rate independent. An improved treatment is the consistent average treatment developed by Öttinger[12], in which the non-equilibrium distribution function is used to average the HI tensor. Regarding curve c as the correct result, it is clear that Öttinger's curve e is better than the pre-averaging result f. The introduction of higher-order HI and EV in the curve, d, of López de Haro and Rubí produces a further improvement. These authors and we have demonstrated that the influence of EV is much more remarkable than that of higher-order terms in HI. Therefore, the decrease in $[\eta]$ from e to d is mostly due to excluded volume. Thus the consistent average procedure predicts that the EV effect should decrease $[\eta]$. This prediction is contrary to the physical intuition, confirmed by our results, that $[\eta]$ should increase. As found in the study of many other related problems in polymer hydrodynamics, the averaging (*a priori* or consistent) of the HI tensor has a serious influence on the predicted dynamics of the model. Nonetheless, the consistent average treatment and its refinements modify the shear rate dependence of the material functions in the correct direction, and seem, therefore, to have a practical validity. The interest of such a treatment is enhanced by its quasi-analytical character.

ACKNOWLEDGEMENTS

This work was supported by grants PR84 0561/84 (J.G.T.) and PB86/0012 (J.J.F.) from CAICYT. We are grateful to Dr M. López de Haro for his comments, which were very helpful in the discussion of the results of this work.

REFERENCES

1 Bird, R. B., Hassager, O., Armstrong, R. C. and Curtiss, C. F. 'Dynamics of Polymeric Liquids', Vol. 2, 'Kinetic theory', Wiley, New York, 1977
2 Yamakawa, H. 'Modern Theories of Polymer Solutions', Harper and Row, New York, 1971
3 Zimm, B. H. *Macromolecules* 1980, **13**, 592
4 García de la Torre, J., Jiménez, A. and Freire, J. J. *Macromolecules* 1982, **15**, 148
5 Ermak, D. L. and McCammon, J. A. *J. Chem. Phys.* 1978, **69**, 1352
6 Fixman, M. *Macromolecules* 1986, **19**, 1195
7 Bird, R. B., Saab, H. H., Dotson, P. J. and Fan, X. J. *J. Chem. Phys.* 1983, **79**, 5729
8 Dotson, P. J. *J. Chem. Phys.* 1983, **79**, 5730
9 Dotson, P. J. Rheology Research Center Report RRC 93, University of Wisconsin, Madison, 1984
10 Saab, H. H. and Bird, R. B. *J. Chem. Phys.* 1987, **86**, 3032
11 Saab, H. H. and Dotson, P. J. *J. Chem. Phys.* 1987, **86**, 3039
12 Öttinger, H. C. *J. Chem. Phys.* 1985, **83**, 6535
13 Öttinger, H. C. *J. Chem. Phys.* 1986, **84**, 4068
14 Öttinger, H. C. *J. Chem. Phys.* 1986, **85**, 1669
15 Kuhn, W. *Kolloid Z.* 1934, **68**, 2
16 Rouse, P. E. *J. Chem. Phys.* 1953, **21**, 1272
17 López de Haro, M. and Rubí, J. M. *J. Chem. Phys.* 1988, **88**, 1248
18 Yamakawa, H. *J. Chem. Phys.* 1970, **53**, 436
19 Rotne, J. and Prager, S. *J. Chem. Phys.* 1969, **50**, 4831

20 García de la Torre, J. and Bloomfield, V. A. *Biopolymers* 1977, **16**, 1747
21 García de la Torre, J. and Bloomfield, V. A. *Q. Rev. Biophys.* 1981, **14**, 81
22 Fan, X. J. *J. Chem. Phys.* 1986, **85**, 6237
23 Pyun, C. W. *J. Chem. Phys.* 1968, **49**, 2875
24 Pyun, C. W. and Fixman, M. *J. Chem. Phys.* 1965, **42**, 3838
25 Allison, S. A. and McCammon, J. A. *Biopolymers* 1984, **23**, 167
26 Dickerson, E. *Chem. Soc. Rev.* 1985, **14**, 421
27 Díaz, F. G., Iniesta, A. and Garcia de la Torre, J. *J. Chem. Phys.* 1987, **87**, 6021
28 Ansell, G. C., Dickman, E. and Ludvigsen, M. *J. Chem. Soc. Trans. Faraday Soc. II* 1985, **81**, 1269
29 Gardiner, C. W. 'Handbook of Stochastic Methods for Physics, Chemistry and the Natural Sciences', Springer, Berlin, 1983
30 Öttinger, H. C. *J. Non-Newtonian Fluid Mech.* 1986, **19**, 357